The 6th Korea-Japan Joint Workshop on Microwave and Millimeter-wave Photonics

MICROWAVE PHOTONICS

Technical Digest

January 27-28, 2005

Hotel Hyundai
Gyeongju, Korea

Sponsored by

From Korea

Optical Communication Technical Group, KICS
Lightwave and Quantum Electronics Group, IEEK
Millimeter-wave Inovation Technology and Research Center, MINT
National Research Laboratory on Microwave Photonics, Yonsei Univ.
Advanced Photonics Technology, MOST

From Japan

Microwave and Millimeter-wave Photonics Technical Group, IEICE
IEEE MTT-S and LEOS Japan Chapters
Japanese Microwave Photonics Committee, IEICE
Japan National Committee of URSI, Commissions C and D

Equivalent Circuit Models for InP/InGaAs HPT

Jae-Young Kim[1], Chang-Soon Choi[1], Hong-Seong Kim[2], Eun-Soo Nam[2] and Woo-Young Choi[1]

[1]Department of Electrical Electronic Engineering, Yonsei University, Seoul, Korea
Tel) +82-2-2123-2874, E-mail) wchoi@yonsei.ac.kr
[2]Electronics and Telecommunications Research Institute (ETRI), Daejun, Korea

***Abstract* —Equivalent circuit models for InP/InGaAs HPT are developed. Particularly, the effects of optical illumination on device parameters are considered. Using the models, the optical modulation responses are evaluated and compared with measurement results. The anomalous behavior that photonic bandwidth of HPT decreases as optical power increases can be explained by the increased base-emitter and base-collector capacitances.**

***Index Terms* — Equivalent model, HPT, modulation response, bandwidth reduction, optical power dependency.**

I. INTRODUCTION

InP/InGaAs Heterojunction Photo-Transistors (HPTs) are very useful devices for radio-on-fiber applications because they provide not only high optical responsivity but also several attractive functions such as optoelectronic mixing and optical injection-locked oscillation [1-2]. In addition, HPTs can be monolithically integrated with HBT without modification of epitaxial layers, which allows simple optoelectronic integrated circuit (OEIC) process [2].

For the design of HPT-based OEIC, equivalent circuit models that include optical illumination effects are required. The object of this paper is to establish equivalent circuit models for HPT and to describe the effect of optical illumination on the model parameters.

The device used in our investigation is InP/InGaAs single-heterojunction N-p-n HPT with base doping of 4×10^{19} cm^{-3} and emitter size of 2x10 um^2. The epitaxial layer structure for the device is shown in Fig. 1.

II. HPT DEVICE CHARACTERIZATION

DC characterization was performed with semiconductor parameter analyzer (HP4145B) with different base currents under dark and illuminated conditions. When top illumination is applied to the optical window located on the top of base layer, the HPT exhibits responsivity of 0.22A/W.

Scattering parameters of HPT under dark and illuminated conditions were measured with a vector network analyzer (HP8722D) from 50MHz to 40GHz. Optical modulation responses were measured with the network analyzer and a directly modulated DFB LD from 50MHz to 13.5GHz frequency range after careful calibration of experimental setup.

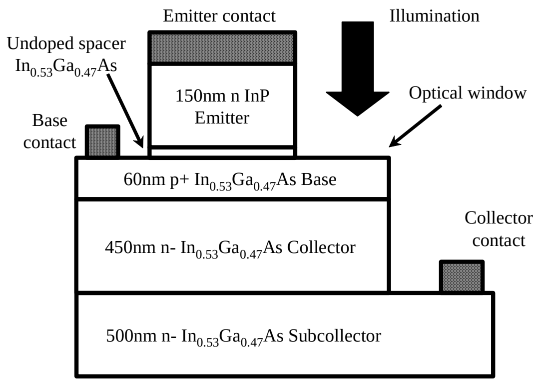

Fig. 1. Schematic diagram of InP/InGaAs HPT used in this work.

III. DC MODELING

A DC model for InP/InGaAs HPT was developed with the slight modification of the conventional Gummel-Poon (GP) BJT model. The GP BJT model describes the transistor operation with four diodes including two in base-emitter junction and two in base-collector junction [3]. For most phototransistor applications, HPT is biased in the forward active condition. Therefore, we only considered one diode in base-collector junction, which represents the recombination currents. The resulting DC model is shown in Fig. 2. The DC model parameters such as I_S, n_f, I_{SE}, n_e, I_{SC} and n_r were extracted from the Gummel plot shown in Fig. 3.

This figure also shows that the forward current gain defined as the ratio of $\mathbf{I_C}$ to $\mathbf{I_B}$ strongly depends on $\mathbf{I_C}$. However, conventional BJT models cannot describe this dependence because they exhibit constant forward current gain all over $\mathbf{I_C}$. Therefore, we employed the exponential relationship between forward current gain and $\mathbf{I_C}$ expressed as [4]

$$\beta_f \propto I_C^{\,N} \qquad (1)$$

where N is a fitting parameter.

The optical illumination effect was modeled by inserting a photo-current source, $\mathbf{I_{ph}}$, between base-collection junction as shown in Fig. 2 [5]. The value of $\mathbf{I_{ph}}$ is determined to be 218μA when the optical illumination is 0 dBm, which is comparable to the directly measured optical responsivity of 0.22A/W

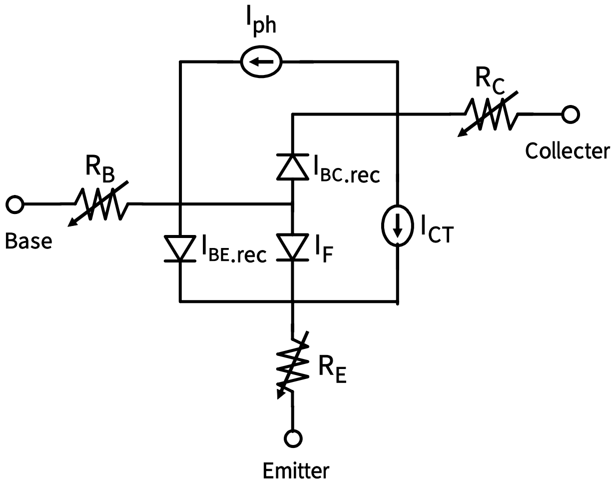

Fig. 2. Developed DC model of InP/InGaAs HPT

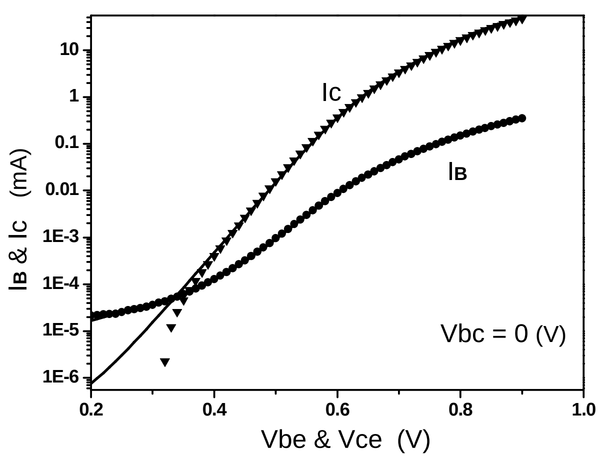

Fig. 3. Gummel plot for measured data (point) and simulation results from the DC model (solid line)

The DC model also includes several extrinsic resistances such as $\mathbf{R_B}$, $\mathbf{R_C}$ and $\mathbf{R_E}$. It is well-known that nonlinear base resistance, $\mathbf{R_B}$, has $\mathbf{I_B}$ dependence, which can be modeled with complex equations [6]. In this work, we used a simpler exponential equation given as

$$R_B = R_{BM} + R_{BB} \times e^{-I_B / A} \qquad (2)$$

where $\mathbf{R_{BM}}$ is the minimum value, and $\mathbf{R_{BB}}$ + $\mathbf{R_{BM}}$ is the maximum value of base resistance. A is the reduction coefficient of base resistance over base current increase. The numerical values for these parameters were obtained by fitting the equation to the value of $\mathbf{R_B}$ determined from small-signal modeling.

Fig. 4 shows $\mathbf{I_C}$-$\mathbf{V_{CE}}$ curves with different $\mathbf{I_B}$ under dark and 0dBm illuminated condition. The slope of $\mathbf{I_C}$ curve in the saturation region is inversely proportional to collector resistance, $\mathbf{R_C}$. It can be observed in this figure that the slope of $\mathbf{I_C}$ is not constant, indicating that $\mathbf{R_C}$ is not a fixed value. Consequently, we modeled $\mathbf{R_C}$ with an exponential function as shown below:

$$R_C = R_{CM} + R_{CC} \times e^{-I_C / B}. \qquad (3)$$

With the nonlinear relationship between extrinsic resistances and terminal currents, our DC model shows good agreement with measured data for wide ranges of base currents and optical illumination powers as shown in fig. 4.

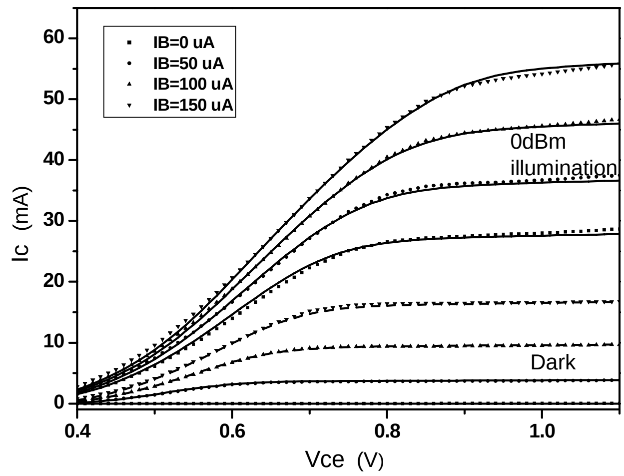

Fig. 4. $\mathbf{I_C}$-$\mathbf{V_{CE}}$ characteristics with different $\mathbf{I_B}$ for dark and 0dBm illumination conditions.

III. AC SMALL-SIGNAL MODELING

Fig. 5 shows the schematic for the AC small-signal model for InP/InGaAs HPT, which is based on the conventional hybrid-π model. The small-signal model parameters were extracted from measured S-parameters by numerical fitting through the optimization process. These were done for $\mathbf{I_B}$ bias points from 0uA to 150μA with 50μA step, in different illuminated optical power conditions. The parasitic components of HPT on-wafer pad structure were eliminated with the de-embedding technique based on open and short test structures [7].

During numerical fitting process, we found that initial values for model parameters are very important to obtain reasonable model parameters. Therefore, we estimated the initial values in the following manner. The developed DC model indicates the approximate values of $\mathbf{R_{BE}}$ and **gm**. It is found that the low frequency value of measured $\mathbf{S_{11}}$ and $\mathbf{S_{22}}$, indicating reflection coefficients of base and collector terminals, are strongly related to $\mathbf{R_{BE}}$ + $\mathbf{R_{BB}}$ and $\mathbf{R_O}$ as expressed by

$$R_{be} + R_{bb} = 50 \times \frac{1+|S_{11}|}{1-|S_{11}|} \quad (4)$$

and $$R_o = 50 \times \frac{1+|S_{22}|}{1-|S_{22}|} \ . \quad (5)$$

From these estimations, we obtained the approximate values of $\mathbf{R_{BE}}$, $\mathbf{R_{BB}}$, $\mathbf{R_O}$ and **gm.** These values were employed as the initial values of parameter optimization process.

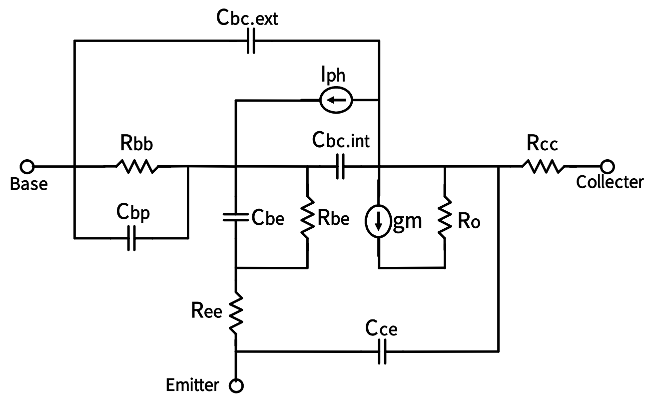

Fig. 5. Schematic of AC small-signal model

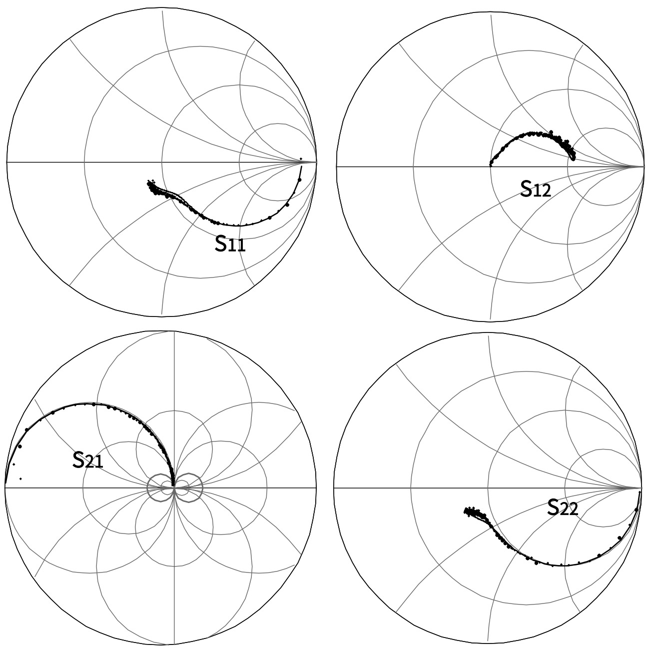

Fig. 6. Comparison of measured and simulated S-parameters biased at $\mathbf{I_B}$ = 100μA and $\mathbf{V_{CE}}$ = 1.0 V

S-parameter simulation results from developed AC small-signal model biased at $\mathbf{I_B}$ = 100μA and $\mathbf{V_{CE}}$ = 1.0 V are compared with measured S-parameters in Fig. 6. From extracted small-signal model parameters with several base currents and optical powers, the dependence of small-signal parameters on input optical power were observed. $\mathbf{R_{BE}}$, $\mathbf{R_O}$ and $\mathbf{R_{BB}}$ are inversely proportional to optical powers, and **Cbe** and **Cbc_int** increase exponentially with optical power. These results are summarized in Table 1.

	Dark	-12dBm	-8dBm	-5dBm	-2dBm
$\mathbf{R_{BB}}$ [Ω]	350	315	290	262	225
$\mathbf{R_{BE}}$ [Ω]	475	434	388	320	103
$\mathbf{R_O}$ [Ω]	7.5 K	5.3 K	4.4 K	2.2 K	1.6 K
$\mathbf{C_{BE}}$ **[fF]**	212	261	303	375	953
$\mathbf{C_{BC\_int}}$ **[fF]**	5.3	6.15	6.8	7	9.1

Table. 1. Optical power dependencies of AC small-signal model parameters biased at $\mathbf{I_B}$ = 100μA and $\mathbf{V_{CE}}$ = 1.0 V

IV. Optical Modulation Response

For the high-speed photo-detection applications, the photonic bandwidth is one of the important parameters. However, our experimental results show that the photonic bandwidth of HPT strongly depends on incident optical powers [8]. The photonic bandwidth is inversely proportional to optical power as shown in Table 2. To analyze this phenomenon, we simulated the optical modulation response with the developed small-signal model.

	-12dBm	-8dBm	-5dBm	-3dBm	-2dBm
$\mathbf{BW_{-3dB}}$ **[GHz]**	1.6	1.32	1.09	0.95	0.8

Table. 2. Optical power dependence of photonic 3dB bandwidth

As shown in Fig. 5, the incident optical signal was modeled by an AC current source between base-collector junction. The detected powers were observed at the collector node. The simulations for optical modulation response were executed for several small-signal models for different optical powers with the fixed bias of $\mathbf{I_B}$ = 100μA and **Vce** = 1.0 V. The comparison between simulated and measured optical modulation responses at optical power of -12, -8 and -5dBm are shown in Fig. 7. Simulation results are well-matched to experimental results at frequencies below 2GHz. However, at higher frequencies, there is some discrepancy.

From modulation response simulation, we found that $\mathbf{C_{BE}}$, $\mathbf{C_{BC\_int}}$, $\mathbf{C_{BC\_ext}}$ and $\mathbf{R_{BE}}$ are the dominant parameters for determining optical modulation response, particularly for optical 3dB bandwidth. Among these parameters $\mathbf{C_{BC\_ext}}$ does not show the optical power dependence, and $\mathbf{R_{BE}}$ is inversely proportional to optical power. On the other hand, $\mathbf{C_{BE}}$ and $\mathbf{C_{BC\_int}}$ exponentially increase in proportion to optical power as shown in fig. 8. Therefore, the bandwidth reduction effect in high incident optical power can be explained by the increased $\mathbf{C_{BE}}$ and $\mathbf{C_{BC\_int}}$.

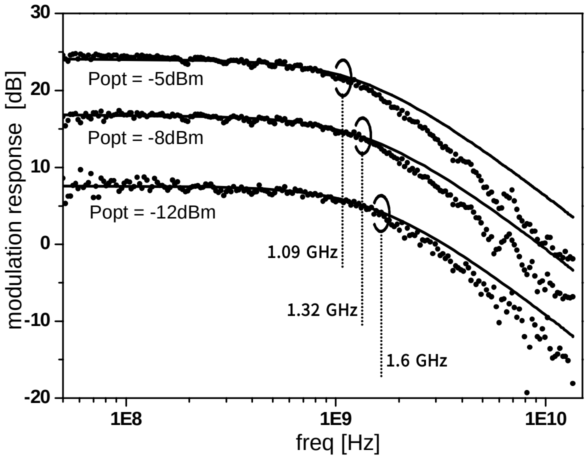

Fig. 7. Comparison of measured and simulated optical modulation responses biased at $\mathbf{I_B}$ = 100μA and **Vce** = 1.0 V

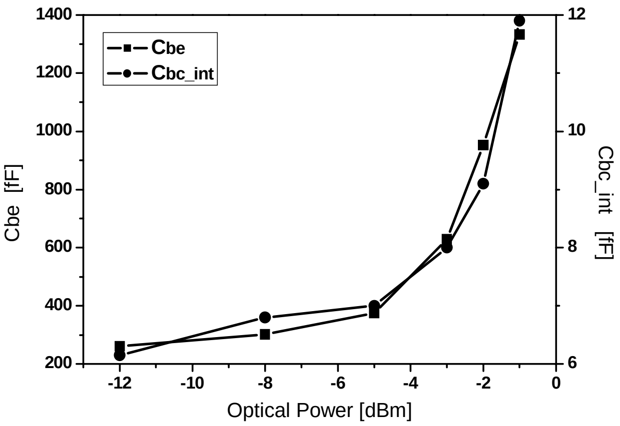

Fig. 8. **Cbe** and **Cbc_int** versus illuminated optical power

V. CONCLUSION

In this paper, equivalent circuit models of InGaAs/InP HPT were developed for DC and AC. The device parameters of developed model can describe the effects of optical illumination. Using the AC small-signal model, the optical modulation responses for HPTs were evaluated and compared with measurement results. In addition, we analyzed the anomalous behavior that photonic bandwidth of HPTs decreases as optical power increases with changes in AC small-signal model parameter values. Based on our model, the photonic bandwidth reduction of HPT in illumination condition can be explained by increased base-emitter and base-collector capacitances.

REFERENCES

[1] Y. Bester, D. Ritter, C. P. Liu, A. J. Seed and A. Madjar, “A Single-Stage Three-Terminal Heterojunction Bipolar Transistor Optoelectronic Mixer,” *IEEE Journal of Lightwave Technology*, vol. 16, No. 4, pp.605 – 609, April 1998

[2] H. Kamitsuna, K. Ishii, T. Shibata, K. Kurishima and M. Ida, “A 43-Gb/s Clock and Data Recovery OEIC Integrating an InP-InGaAs HPT Oscillator with an HBT Decision Circuit,” *IEEE Journal of selected Topics in Quantum Electronics*, vol. 10, No. 4, pp.673 – 678, July/August 2004

[3] M. E. Hafizi, C. R. Crowell and M. E. Grupen, “The DC Characteristics of GaAs/AlGaAs Heterojunction Bipolar Transistors with Application to Device Modeling,” *IEEE Trans. on Electron Devices*, vol. 37, No. 10, pp.2121-2129, October 1990.

[4] Ke Lu, P. A Perry and T. J. Brazil, “ A New Large-Signal AlGaAs/GaAs HBT Model Including Self-Heating Effects, with Corresponding Parameter-Extraction Procedure,” *IEEE Trans. on MTT*, vol. 43, No. 7, pp.1433-1445, July 1995.

[5] S. M. Frimel and K. P. Roenker, “Gummel-Poon model for Npn heterojunction bipolar phototransistors, *J. Appl. Phys*. pp.3581-3592, October 1997.

[6] M. Linder, F. Ingvarson, K. O. Jeppson, J. V. Grahn, S. L. Zhang and M. Ostling, “On DC Modeling of Base Resistance in Bipolar Transistors,” *Solid-State Electronics*, vol. 44, pp.1411-1418. 2000.

[7] D. Costa, W. U. Liu and J. S. Harris, “Direct Extraction of the AlGaAs/GaAs Heterojunction Bipolar Transistor Small-Signal Equivalent Circuir,” *IEEE Trans. on Electron Devices*, vol. 38, No. 9, pp.2018-2024, September 1991.

[8] K. Teshima, H. Kamitsuna, M. Ida, K. Kurishima and M. Akaike, “Analysis of the Equivalent Circuit Parameters in Low Collector Current of an Illuminated HPT,” *J. K. Jiont Workshop on Microwave and Millimeter-wave Photonics*, T4-13, pp.91-94, 2004